

# Soft-mode spectroscopy of the improper ferroelastics $\text{Hg}_2\text{Cl}_2$ and $\text{Hg}_2\text{Br}_2$

B. S. Zadokhin, Yu. F. Markov, and A. S. Yurkov

*A. F. Ioffe Physicotechnical Institute, Russian Academy of Sciences*

*194021 St. Petersburg, Russia*

(Submitted 15 February 1993)

Zh. Eksp. Teor. Fiz. **104**, 2799–2814 (August 1993)

We have performed accurate temperature studies of the parameters of the soft mode [frequency, half-width, and intensity of the corresponding line of the Raman scattering spectrum (RSS)] in  $\text{Hg}_2\text{Cl}_2$  and  $\text{Hg}_2\text{Br}_2$  single crystals over a wide temperature range (100–300 K), including the phase-transition point. Above the phase-transition point the temperature dependence of the frequency of the soft mode at the  $X$  point of the Brillouin zone of the paraphase is described by a power-law function with the critical exponents  $\beta' = 0.50 \pm 0.02$  ( $\text{Hg}_2\text{Cl}_2$ ) and  $\beta' = 0.51 \pm 0.02$  ( $\text{Hg}_2\text{Br}_2$ ). At temperatures  $T \leq T_c$  the temperature dependence of the frequency of the soft mode is not described by a simple power-law function. The resulting characteristics of the soft mode show that the phase transition in  $\text{Hg}_2\text{Cl}_2$  and  $\text{Hg}_2\text{Br}_2$  is close to the triple point. The model proposed for the phase transition explains the temperature dependence of the soft-mode frequency and the temperature dependence of the intensity of the RSS spectrum both above and below the phase-transition temperature. The shape of the second-order RSS line is described successfully on the basis of a quadratic phonon dispersion law near the  $X$  point of the Brillouin zone. Anomalous behavior of the frequency and integral intensity of the RSS of the soft mode as  $T \rightarrow T_c^-$  was observed close to the phase transition. This anomaly can be explained by the interaction of the soft mode and a relaxation mode.

Monovalent mercury halides  $\text{Hg}_2\text{X}_2$  ( $X = \text{Cl}, \text{Br}$ ) at room temperature have a unique crystalline structure, consisting of weakly coupled chains of parallel linear molecules  $X\text{-Hg-Hg-X}$  (symmetry space group  $D_{4h}^{17}$  with one molecule per unit cell). The simplicity of the crystalline structure, combined with the well defined effects of a phase transition (PT) make monovalent mercury halides convenient model objects for studying the general problems of structural phase transitions in crystals.<sup>1</sup>

On the basis of investigations of PT effects in first-order Raman scattering spectra (RSS), including observation of a soft mode, reaching extremely low frequencies<sup>2</sup>  $\sim 2 \text{ cm}^{-2}$  as  $T \rightarrow T_c^-$  ( $T_c = 186 \text{ K}$  for  $\text{Hg}_2\text{Cl}_2$  and  $144 \text{ K}$  for  $\text{Hg}_2\text{Br}_2$ ) below  $T_c$ , Barta *et al.*<sup>3</sup> concluded that the phase transition  $D_{4h}^{17} \rightarrow D_{2h}^{17}$  in  $\text{Hg}_2\text{X}_2$  is induced by a soft  $TA$  mode at the  $X$  point of the Brillouin zone of the tetragonal phase and is accompanied at temperatures  $T \leq T_c$  by doubling of the unit cell. Further detailed experimental investigations of PT effects in second-order RSS (in particular, observation for  $T > T_c$  of a soft mode at the boundary of the Brillouin zone)<sup>4</sup> and IR spectra<sup>5</sup> as well as the group-theoretical analysis performed in Refs. 4 and 5 are in complete agreement with the conclusion drawn in Ref. 3 concerning the nature of the PT in  $\text{Hg}_2\text{X}_2$ . The validity of this result was confirmed unequivocally in subsequent x-ray<sup>6</sup> and neutron<sup>7</sup> diffraction studies.

The structural phase transition  $D_{4h}^{17} \rightarrow D_{2h}^{17}$  was studied on the basis of the Landau phenomenological theory of second-order phase transitions.<sup>3</sup> The thermodynamic potential with a two-component order parameter was constructed<sup>8</sup> taking into account the nonlinear (strictional) interaction of the order parameter with the defor-

mation and used to determine the theoretical temperature dependence of the soft-mode frequency above and below  $T_c$ . However, the experimental temperature dependence  $\nu_{\text{SM}}(T)$  below  $T_c$  (Refs. 2 and 3) does not fit within the Landau's phenomenological theory of second-order phase transitions. It was conjectured that these discrepancies could be due, in part, to enhancement of fluctuations near a phase transition. It should be noted that high-precision measurements of  $\nu_{\text{SM}}(T)$  were not performed in Refs. 2 and 3.

In the present work we performed accurate temperature studies of the soft-mode parameters (frequency, half-width, and intensity of the corresponding lines in the RSS) in  $\text{Hg}_2\text{Cl}_2$  and  $\text{Hg}_2\text{Br}_2$  single crystals over a wide temperature range (100–300 K), including the PT point. The soft-mode characteristics obtained show that the PT in  $\text{Hg}_2\text{Cl}_2$  and  $\text{Hg}_2\text{Br}_2$  is close to the triple point, in agreement with the results of experimental investigations of the heat capacity and spontaneous deformation in  $\text{Hg}_2\text{X}_2$  (Refs. 9 and 10).

Anomalous behavior of the frequency and integral intensity of the soft-mode RSS as  $T \rightarrow T_c^-$  was observed close to the phase-transition point.

## 1. EXPERIMENTAL RESULTS

It is well known<sup>3</sup> that in the paraphase ( $T > T_c$ ) of monovalent mercury halides the soft mode is a  $TA$  vibration at the  $X$  point of the Brillouin zone of the paraphase. When this mode condenses ( $T \leq T_c$ ), the  $X$  point of the paraphase is transformed into the  $\Gamma$  point of the Brillouin zone of the ferroelectric phase. For this reason, new lines, including also the soft-mode line, which is observed below

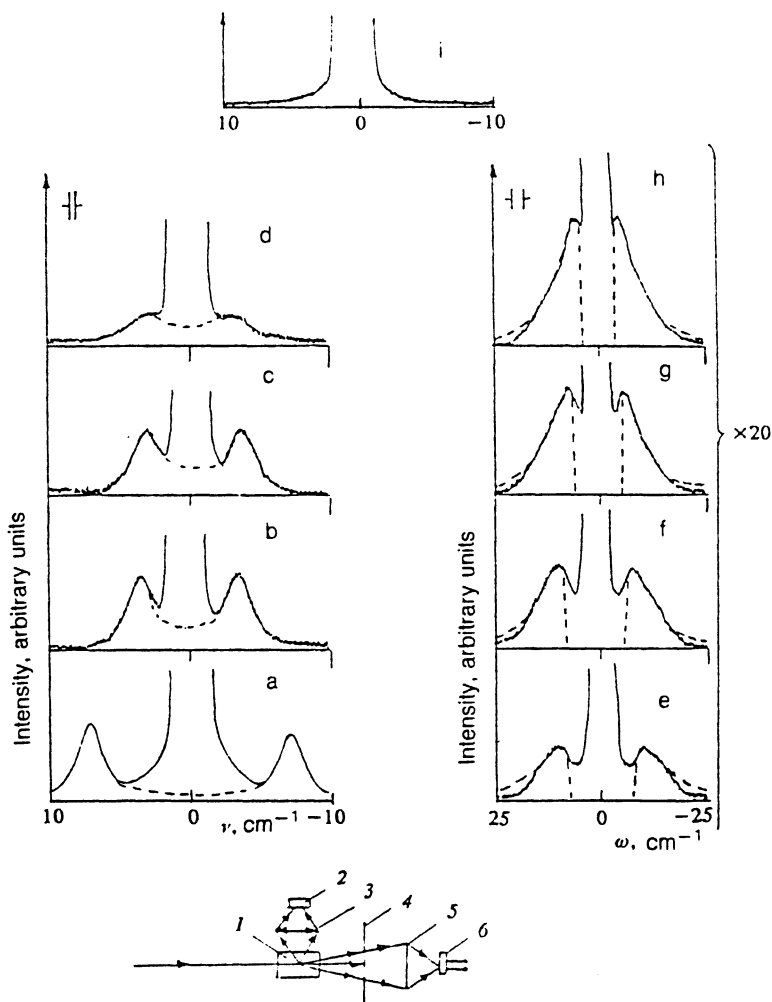


FIG. 1. Soft-mode Raman-spectra of  $\text{Hg}_2\text{Cl}_2$  crystals at different temperatures: a)  $T=170.3$  K; b)  $T=185.6$  K; (b, c)  $T=185.8$  K; d)  $T=185.9$  K; e)  $T=186.0$  K; f)  $T=206.5$  K; g)  $T=217.6$  K; h)  $T=242.7$  K; and, i)  $T=261.4$  K. The dashed line represents the computed RS spectrum of the soft mode. A) Experimental arrangement used to record the RSS and small-angle scattering: 1—sample; 2—screen; 3, 5—lenses; 4—photodetector; 6—spectrometer slit.

$T_c$  as a low-frequency narrow line, whose frequency  $\nu_{\text{SM}}$  becomes quite low as  $T \rightarrow T_c^-$ ,<sup>1)</sup> appear in the first-order RSS. In this connection, the soft-mode RSS was investigated using a Dilor Z-24 triple Raman spectrometer, having a very low level of scattered light, with an  $\text{Ar}^+$  laser ( $\lambda=5145 \text{ \AA}$ ). An iodine filter was employed, which made it possible to further reduce the Rayleigh scattering background near the exciting line. The power of the  $\text{Ar}^+$  laser beam on the sample was less than 20 mW. This low power level made it possible to reduce local heating to a minimum. With the same aim, measurements of the RSS of  $\text{Hg}_2\text{Br}_2$  single crystals were performed with the help of a  $\sim 10$  mW He-Ne laser. The investigated samples were placed in a specially constructed optical cryostat through which nitrogen gas was blown and in which the temperature could be regulated continuously. The temperature was determined with an accuracy of  $\approx 0.05$  K.

The soft-mode RSS was investigated simultaneously in the anti-Stokes and Stokes regions in the spectral range  $-25$ – $+25 \text{ cm}^{-1}$  on oriented  $\text{Hg}_2\text{X}_2$  single crystals in  $z(xx)y$  geometry; this made it possible to measure small-angle light scattering at the same time that the soft-mode RSS was recorded.<sup>11</sup> The experimental arrangement employed for recording the RSS and the small-angle scattering is displayed in Fig. 1a. Figures 1 (a, b, c, and d) and 2 (a, b, c, and d) display, respectively, the soft-mode RSS of  $\text{Hg}_2\text{Cl}_2$  and  $\text{Hg}_2\text{Br}_2$  at different temperatures ( $T < T_c$ ).

The dashed curves represent the soft-mode RSS obtained with the help of the formula

$$I(\nu) = I_{\text{SM}}(\nu) + h_R I_R(\nu) + h_b I_b, \quad (1)$$

where  $I_{\text{SM}}(\nu)$  is the spectral density of the light intensity, corresponding to first-order Raman scattering of the soft mode;  $I_R(\nu)$  is the spectral density of Rayleigh scattering;  $I_b$  is the background; and,  $h_R$  and  $h_b$  are constants.

In the damped harmonic oscillator model the spectral density of the intensity of the first-order soft-mode RSS is determined by a formula<sup>12</sup> describing simultaneously the Stokes and anti-Stokes components of the RSS:

$$I_{\text{SM}}(\nu) = [I + n(\nu)] A_1 \Gamma_{\text{SM}} \nu_{\text{SM}} / [(\nu_{\text{SM}}^2 - \nu^2)^2 + \Gamma_{\text{SM}}^2 \nu^2], \quad (2)$$

where  $\Gamma_{\text{SM}}$  and  $\nu_{\text{SM}}$  respectively are the damping and frequency of the soft mode;  $n(\nu)$  is the Bose-Einstein factor, which is equal to  $kT/\hbar\nu$  in the classical approximation ( $kT \gg \hbar\nu$ ); and  $\nu = \nu_i - \nu_f$ , where  $\nu_i$  and  $\nu_f$  are the frequencies of the incident and scattered light respectively. The quantity  $A_1$  is the product of the incident radiation power, the squared parameter of the linear photon-phonon interaction, a geometric factor depending on the scattering volume, the angular aperture of the spectrometer, and so on. Since the soft-mode RSS was measured in arbitrary units (see Figs. 1 and 2), we assume that  $A_1$  is the squared photon-phonon interaction parameter, because the other

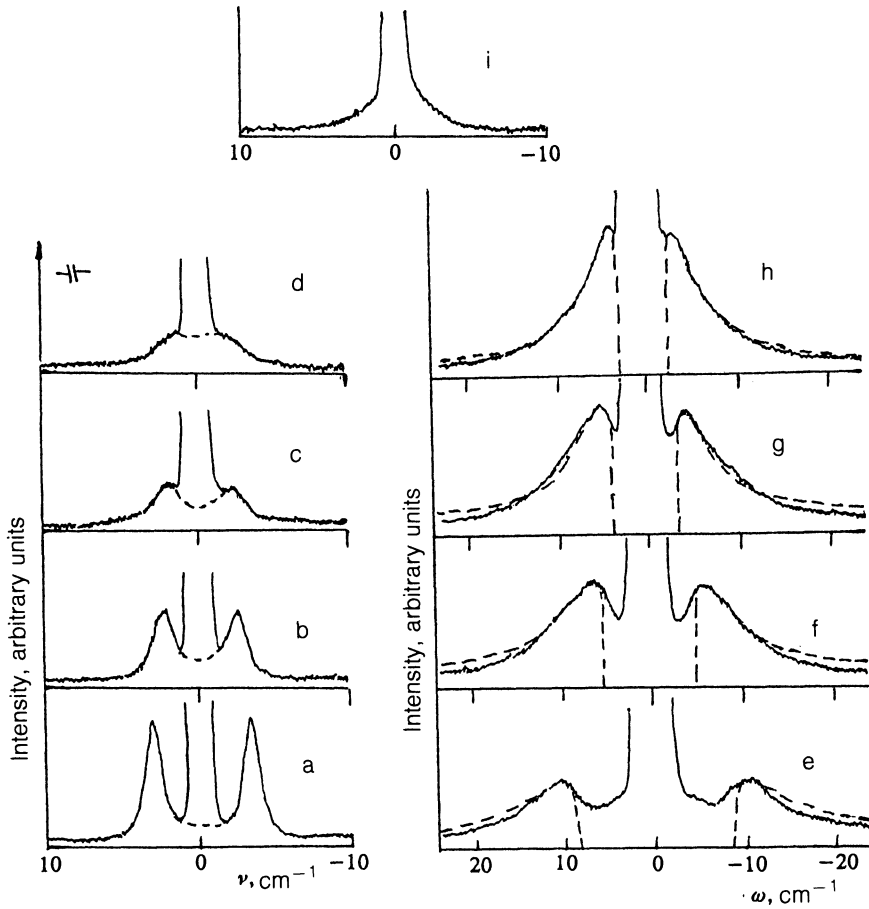


FIG. 2. Soft-mode Raman spectra of  $\text{Hg}_2\text{Br}_2$  crystals at different temperatures: a)  $T=141.7$  K; b)  $T=143.3$  K; c)  $T=143.6$  K; d)  $T=143.7$  K; e)  $T=144.0$  K; f)  $T=157.5$  K; g)  $T=166.8$  K; h)  $T=182.5$  K; and, i)  $T=263.0$  K. The dashed line represents the computed RS spectrum of the soft mode.

factors appearing in  $A_1$  remained unchanged in the course of the experiment. It is convenient to determine  $A_1$  in terms of the integrated intensity of the RSS of the soft mode:

$$A_1 = (\hbar/\pi kT) v_{\text{SM}}^2 I_{\text{SM}}^{\text{int}}, \quad (3)$$

where  $I_{\text{SM}}^{\text{int}} = \int_{-\infty}^{\infty} I_{\text{SM}}(\nu) d\nu$ .

Since Rayleigh scattering significantly affects the soft-mode RSS only near a phase-transition point [ $\Delta T = T_c - T < 5$  K for  $\text{Hg}_2\text{Cl}_2$  and  $< 2$  K for  $\text{Hg}_2\text{Br}_2$ ; see Figs. 1 and 2 (b, c, d)], the intensity of the Rayleigh line at the phase-transition point [Figs. 1 and 2 (e)] was used for  $I_R$  in the calculations. In so doing, it was assumed that  $I_R$  does not depend significantly on the temperature.

Five parameters were used as adjustable parameters in order to analyze the soft-mode RSS with the help of Eq. (1):  $A_1$ ,  $\Gamma_{\text{SM}}$ ,  $\nu_{\text{SM}}$ ,  $h_R$ , and  $h_b$ . The parameters were chosen so as to obtain the best agreement between the experimental and computed RSS of the soft mode (dashed line in Figs. 1 and 2). When Eq. (1) is used (the Stokes and anti-Stokes components of the RSS are determined at the same time), the value of the most important characteristic of the soft mode—the frequency—is determined most accurately. In our work the frequency of the soft mode was determined to within  $\pm 0.1 \text{ cm}^{-1}$ . Other characteristics of the soft mode were also determined: the integral intensity  $I_{\text{SM}}^{\text{int}}$  and the damping  $\Gamma_{\text{SM}}$ .

In investigations of the soft-mode RSS certain difficulties usually arise in determining the phase-transition tem-

perature  $T_c$ , because as  $T \rightarrow T_c$  the line corresponding to the soft mode generally becomes weaker and the soft mode becomes overdamped, making it difficult to distinguish the soft mode against the background Rayleigh line. As a reference for  $T_c$  we employed the small-angle light scattering, which makes it possible to record the moment of the phase transition accurately.<sup>11</sup>

The temperature dependences of the frequency (a) and the integral intensity  $I_{\text{SM}}^{\text{int}}$  (b) of the soft mode and the intensity  $I_{\text{SALS}}$  (c) near the phase transition point are presented in Fig. 3 for  $\text{Hg}_2\text{Cl}_2$  (Fig. 3a) and  $\text{Hg}_2\text{Br}_2$  (Fig. 3b) single crystals. As  $T \rightarrow T_c^-$  the frequency of the soft mode practically does not change and it remains finite:  $\sim 3.5 \text{ cm}^{-1}$  for  $\text{Hg}_2\text{Cl}_2$  and  $\sim 2.5 \text{ cm}^{-1}$  for  $\text{Hg}_2\text{Br}_2$ . As  $I_{\text{SM}}^{\text{int}} \rightarrow 0$  the intensity  $I_{\text{SALS}}$  at the PT point has a pronounced maximum associated with strong diffuse scattering of light caused at  $T \approx T_c$  by the “chaotic” state of in the experimental crystals.<sup>11</sup> Some samples employed for measuring the RSS and small-angle scattering consisted of  $\text{Hg}_2\text{Cl}_2$  and  $\text{Hg}_2\text{Br}_2$  single crystals on which measurements of the heat capacity  $C_p$  were performed by the method of adiabatic calorimetry.<sup>9,10</sup> The intensities  $I_{\text{SM}}^{\text{int}}$  and  $I_{\text{SALS}}$  measured on these samples are displayed in Fig. 3 (crosses). The figure also displays the experimental values of the heat capacity  $C_p$  from Refs. 9 and 10 [Figs. 3a and b (d)]. The maximum of  $C_p$ , the maximum of  $I_{\text{SALS}}$ , and the moment at which the line corresponding to the soft mode vanishes ( $I_{\text{SM}}^{\text{int}} = 0$ ) all occur within 0.1 K of one another. On the basis of these

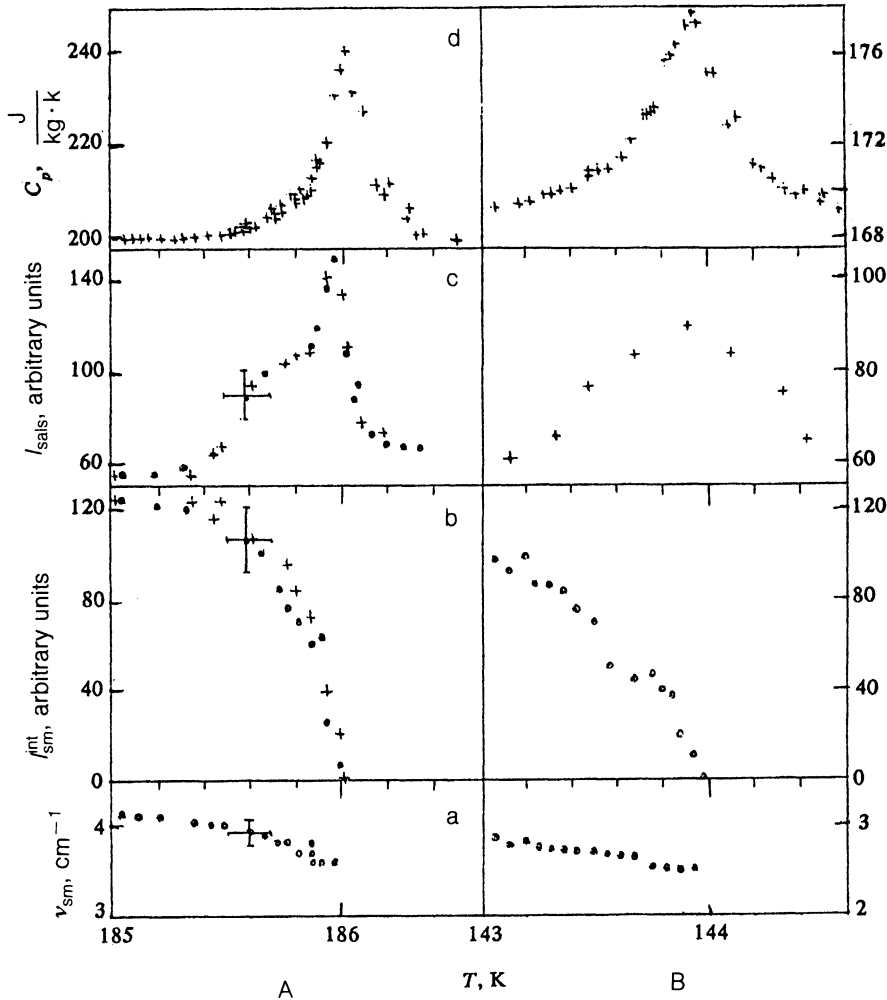


FIG. 3. Temperature dependence of the soft-mode frequency  $\nu_{SM}$  (a), the soft-mode intensity  $I_{SM}^{int}$  (b), the small-angle scattering intensity  $I_{SALS}$  (c), and the heat capacity  $C_p$  (d) of  $Hg_2Cl_2$  (A) and  $Hg_2Br_2$  (B) crystals near the phase-transition point.

measurements we determined the temperature of the phase transition to be  $T_c = 186.0 \pm 0.1$  K for  $Hg_2Cl_2$  and  $144.0 \pm 0.1$  K for  $Hg_2Br_2$ .

Above  $T_c$  the soft mode is a  $TA$  vibration at the  $X$  point of the Brillouin zone of the paraphase. First-order light scattering by this vibration is forbidden by wave-vector selection rules. The soft mode nonetheless appears in the second-order RSS, which is determined by the phonon states from the entire Brillouin zone.<sup>4</sup> For this reason, phonon dispersion must be taken into account at temperatures  $T > T_c$ . The spectral intensity of the second-order RSS is determined by the formula

$$I_{SM}(\omega) \sim [I + n(\omega/2)]^2 \omega^{-2} D(\omega/2), \quad (4)$$

where  $D(\omega)$  is the single-phonon density of states.

In Ref. 7 it is shown that in  $Hg_2Cl_2$  the dispersion of the soft mode near the  $X$  point of the Brillouin zone of the tetragonal phase is described satisfactorily by a quadratic function  $\omega_{SM}^2(q) = \omega_0^2 + \lambda_1 q_1^2 + \lambda_2 q_2^2 + \lambda_3 q_3^2$ , where the wave vector  $q$  is measured from the  $X$  point of the Brillouin zone and  $\lambda_1, \lambda_2, \lambda_3 > 0$  are parameters of the dispersion of the soft mode in the directions, respectively,  $X-\Delta-\Gamma$ ,  $X-E-Z$ , and  $X-W-P$  ( $\Gamma, \Delta, X, E, W, P$ , and  $Z$  are singular points of the Brillouin zone). In this case the density of states has the form

$$D(\omega) \sim \begin{cases} \omega [(\omega^2 - \omega_x^2)/(\lambda_1 \lambda_2 \lambda_3)]^{1/2} & \text{for } \omega > \omega_x, \\ 0 & \text{for } \omega < \omega_x, \end{cases} \quad (5)$$

where  $\omega_x$  is the phonon frequency at the  $X$  point of the Brillouin zone. Since  $\lambda_1 \ll \lambda_2, \lambda_3$  holds according to Ref. 7, vibrations with wave vector in the direction  $X-\Delta-\Gamma$  of the Brillouin zone are mainly manifested in the second-order RSS.<sup>4</sup>

Thus the spectral intensity of lines in the second-order RSS of the soft mode at the  $X$ -point of the Brillouin zone in  $Hg_2X_2$  is determined by

$$I_x(\omega) = A_2 [I + n(\omega/2)]^2 \omega^{-1} [\omega^2 - (2\omega_x)^2]^{1/2}, \quad (6)$$

where  $A_2 = \text{const}$ , which is determined in terms of the integral intensity  $I_x^{int}$  of the second-order RSS as follows:

$$A_2 = (\hbar/2\pi k^2 T^2) \omega_x I_x^{int}, \quad (7)$$

where  $I_x^{int} = \int_{-\infty}^{\infty} I_x(\omega) d\omega$ .

The second-order RSS of the soft mode of, respectively,  $Hg_2Cl_2$  and  $Hg_2Br_2$  at different temperatures above  $T_c$  are displayed in Figs. 1 and 2 (f, g, h, i). The dashed line represents the soft-mode RSS obtained with the help of Eq. (1), where  $I_x(\omega)$  is given by Eq. (6). It should be

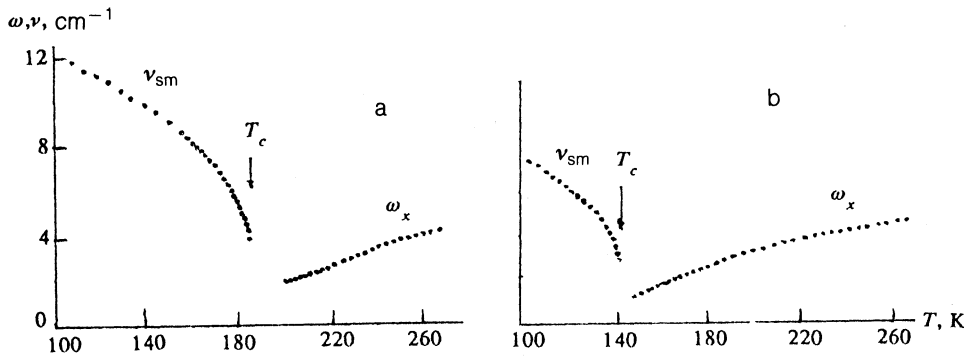


FIG. 4. Temperature dependence of the soft-mode frequency  $\nu_{SM}$  ( $T < T_c$ ) and  $\omega_x$  ( $T > T_c$ ) of  $Hg_2Cl_2$  (a) and  $Hg_2Br_2$  (b) crystals.

noted that in this case the doubled soft-mode frequency at the X point ( $2\omega_x$ ) is different from the frequency of the intensity maximum observed in the second-order soft-mode RSS ( $\omega_{max} = 1.5^{1/2} \cdot \omega_x$ ) (see Figs. 1 and 2).

Figure 4 displays the temperature dependence of the frequency  $\nu_{SM}$  and the frequency  $\omega_x$  obtained for  $Hg_2Cl_2$  (a) and  $Hg_2Br_2$  (b) crystals from the first- and second-order RSS. The frequency  $\omega_x$  as a function of the reduced temperature  $t = (T - T_c) / T_c$  for  $T > T_c$  is presented in Fig. 5 in a log-log plot. In the temperature ranges  $6.45 \cdot 10^{-2} < t < 0.46$  ( $Hg_2Cl_2$ ) and  $6.17 \cdot 10^{-2} < t < 0.8$  ( $Hg_2Br_2$ ) the experimental points are fit well by a straight line. This makes it possible to approximate the temperature dependence of the soft-mode frequency by the formula

$$\omega_x = gt^\beta \quad (8)$$

and the exponents were found by the least-squares method to be  $\beta' = 0.50 \pm 0.02$  ( $Hg_2Cl_2$ ) and  $0.51 \pm 0.02$  ( $Hg_2Br_2$ ). The values of the coefficient  $g$  were also determined:  $6.1 \text{ cm}^{-1}$  ( $Hg_2Cl_2$ ) and  $4.8 \text{ cm}^{-1}$  ( $Hg_2Br_2$ ). In the temperature ranges  $t < 6.45 \cdot 10^{-2}$  ( $Hg_2Cl_2$ ) and  $t < 6.17 \cdot 10^{-2}$  ( $Hg_2Br_2$ ) the experimental points deviate systematically from a straight line in the direction of a weaker temperature dependence of  $\omega_x$ .

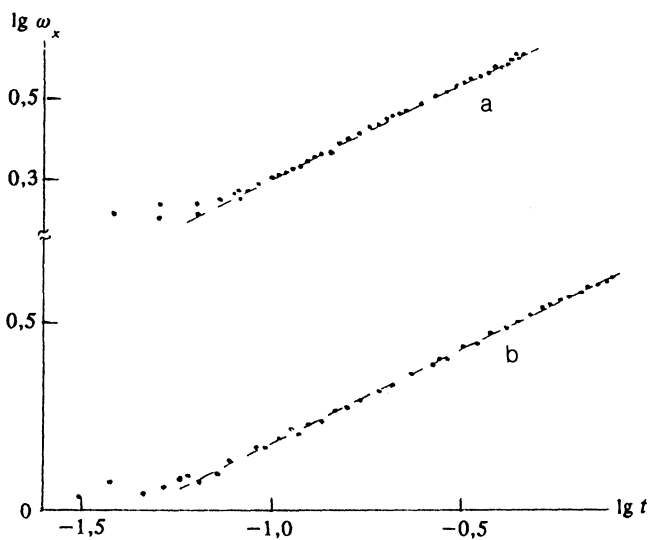


FIG. 5. Log-log plot of the soft-mode frequency  $\omega_x$  versus the reduced temperature  $t$ :  $Hg_2Cl_2$  (a) and  $Hg_2Br_2$  (b).

A log-log plot of the temperature dependence of  $\nu_{SM}$  at temperatures  $T < T_c$  is shown in Fig. 6. It is obvious from this figure that, in contrast to the temperature dependence of the soft-mode frequency above  $T_c$ , the temperature dependence of the soft-mode frequency is not described by a power law over the entire temperature interval of the measurements ( $\Delta T \sim 85 \text{ K}$  for  $Hg_2Cl_2$  and  $\Delta T \sim 45 \text{ K}$  for  $Hg_2Br_2$ ). In this case the experimental points are described well by the formula

$$\nu_{SM}^2 = b_0 + b_1(T_c - T)^{1/2} + b_2(T_c - T), \quad (9)$$

where the least-squares values of the coefficients are as follows:  $b_0 = 10 \text{ cm}^{-2}$ ,  $b_1 = 7.3 \text{ cm}^{-2} \cdot \text{K}^{-1/2}$ ,  $b_2 = 0.80 \text{ cm}^{-2} \cdot \text{K}^{-1}$ ,  $T_c = 186.0 \text{ K}$  ( $Hg_2Cl_2$ );  $b_0 = 3.8 \text{ cm}^{-2}$ ,  $b_1 = 4.3 \text{ cm}^{-2} \cdot \text{K}^{-1/2}$ ,  $b_2 = 0.58 \text{ cm}^{-2} \cdot \text{K}^{-1}$ ,  $T_c = 144.1 \text{ K}$  ( $Hg_2Br_2$ ).

Figure 7 displays the temperature dependence of the soft-mode damping  $\Gamma_{SM}$  below  $T_c$  for  $Hg_2Cl_2$  (a) and  $Hg_2Br_2$  (b). As the temperature changes, the damping  $\Gamma_{SM}$  increases linearly. Close to the phase-transition point ( $\Delta T < 0.2 \text{ K}$  for  $Hg_2Cl_2$  and  $< 0.5 \text{ K}$  for  $Hg_2Br_2$ )  $\Gamma_{SM}$  increases

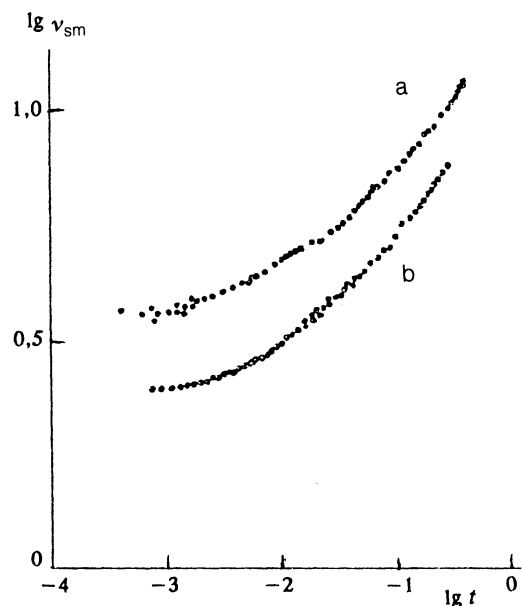


FIG. 6. Log-log plot of the soft-mode frequency  $\nu_{SM}$  versus the reduced temperature  $t$ :  $Hg_2Cl_2$  (a) and  $Hg_2Br_2$  (b).

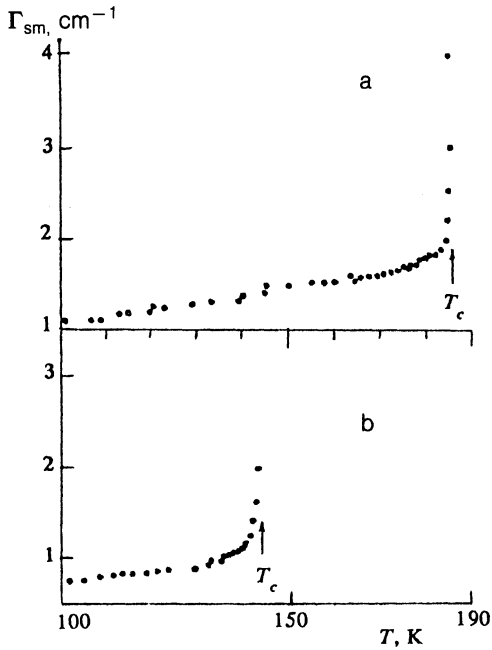


FIG. 7. Temperature dependence of soft-mode damping  $\Gamma_{SM}$  in  $Hg_2Cl_2$  (a) and  $Hg_2Br_2$  (b) crystals.

nonlinearly. However, the experimentally observed soft mode does not become overdamped ( $\Gamma_{SM} < 2^{1/2} \nu_{SM}$ ).

Figure 8 displays the temperature dependence of  $I_{SM}^{int}$  ( $T < T_c$ ) and  $I_X^{int}$  ( $T > T_c$ ) for  $Hg_2Cl_2$  (a) and  $Hg_2Br_2$  (b) crystals.

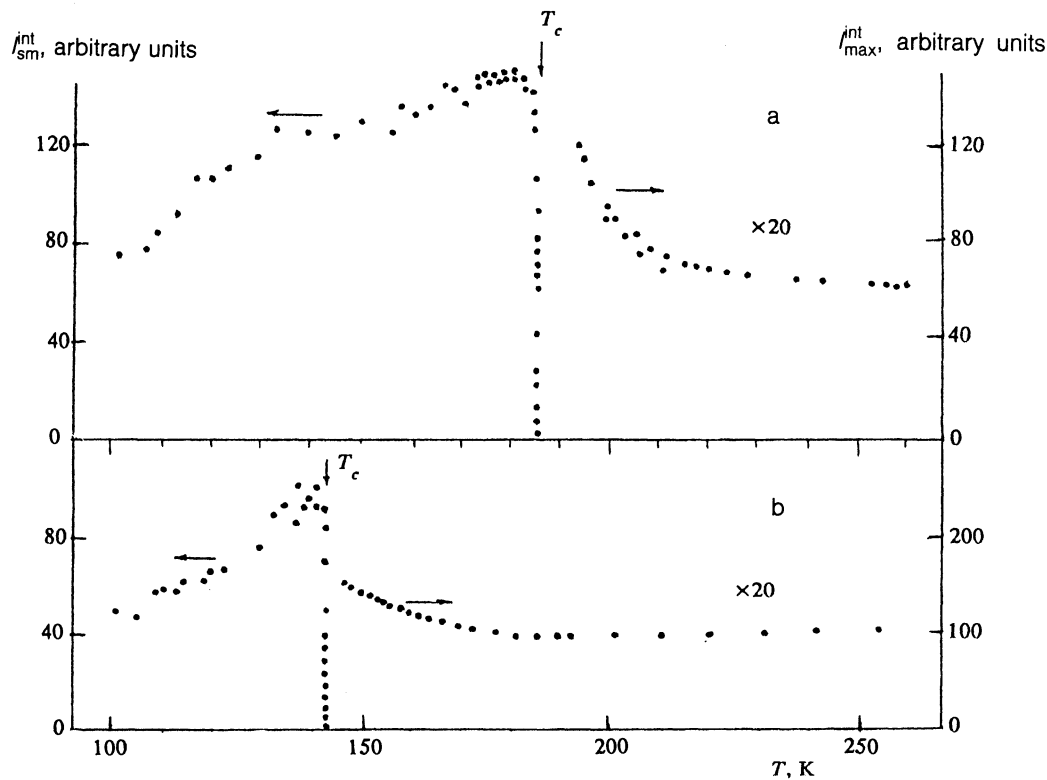


FIG. 8. Temperature dependence of the total RSS intensity  $I_{SM}^{int}$  ( $T < T_c$ ) of the soft mode and the intensities of the maximum of the second-order RSS  $I_{max}^{int}$  ( $T > T_c$ ) of  $Hg_2Cl_2$  (a) and  $Hg_2Br_2$  (b) crystals.

(b). As the temperature decreases,  $I_X^{int}$  increases nonlinearly as  $T \rightarrow T_c^+$ . At temperatures  $T < T_c$  the soft-mode appears in the first-order RSS: At first the intensity of the soft mode  $I_{SM}^{int}$  increases rapidly over a narrow temperature interval ( $\Delta T \sim 2$  K for  $Hg_2Cl_2$  and  $\sim 1$  K for  $Hg_2Br_2$ ), and then away from the phase-transition point it decreases. Note that the intensity of the second-order soft-mode RSS above  $T_c$  is one or two orders of magnitude lower than the soft-mode intensity below the phase-transition point.

## 2. DISCUSSION

We now consider the behavior of the soft mode within the Landau phenomenological theory for different types of phase transitions. For pure improper ferroelastics near the phase transition point the Landau thermodynamic potential can be written as a series in power of the small order parameter (for our purposes it is sufficient to consider the case of single-component order parameter interacting with one component of the elastic strain tensor):<sup>12</sup>

$$\Phi = \Phi_0 + A\rho^2/2 + \beta_1\rho^4/4 + G\rho^6/6 + K\rho^2\varepsilon + C\varepsilon^2/2, \quad (10)$$

where  $\Phi_0$  is the thermodynamic potential of the paraphase;  $\beta_1$ ,  $G$ , and  $K$  are elastic constants;  $\varepsilon$  is the lattice strain;  $C$  is the modulus of elasticity; and  $\rho$  is the equilibrium value of the order parameter. The simplest linear temperature dependence  $A = \lambda(T - T_c)$ , is chosen for the coefficient of  $\rho^2$ . After the functional (10) is minimized with respect to  $\varepsilon$  the thermodynamic potential assumes the form

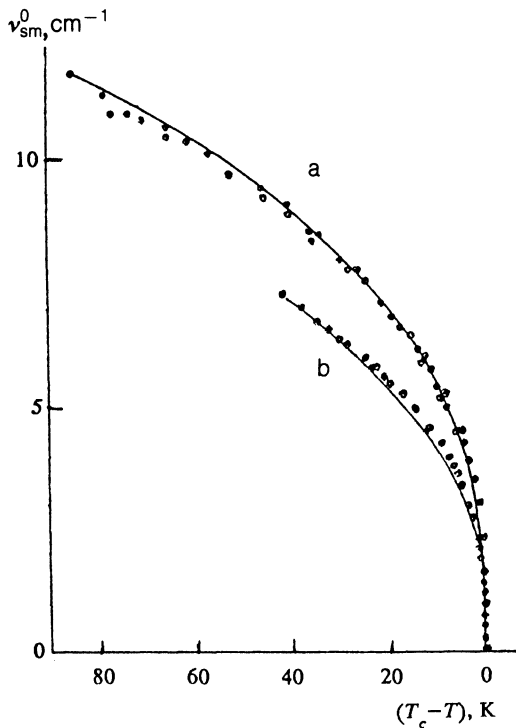


FIG. 9. Temperature dependence of the soft-mode frequency of  $\text{Hg}_2\text{Cl}_2$  (a) and  $\text{Hg}_2\text{Br}_2$  (b) crystals. The dots are the experimental points and the solid line was computed theoretically.

$$\Phi = \Phi_0 + A\rho^2/2 + \gamma_1\rho^4/4 + G\rho^6/6, \quad (11)$$

$$\gamma_1 = \beta_1 - (2K^2)/C.$$

The temperature dependence of the order parameter is then written as

$$\rho^2 = \{[\gamma_1^2 + 4\lambda G(T_c - T)]^{1/2} - \gamma_1\} / (2G). \quad (12)$$

The temperature dependence of the soft-mode frequency will have the form

$$\begin{aligned} \nu_0^2 &= (1/M)(\partial^2\Phi/\partial\rho^2) \\ &= \begin{cases} (\lambda/M)(T - T_c) & \text{for } T > T_c, \\ (2/M)\rho^2(\beta_1 + 2G\rho^2) & \text{for } T < T_c, \end{cases} \quad (13) \end{aligned}$$

where  $M$  is the "mass" of the soft mode.

For a second-order phase transition far from the triple point  $\gamma_1^2 \gg 4\lambda G(T_c - T)$  the temperature dependence of the order parameter is given by the law

$$\rho^2 = (\lambda/\gamma_1)(T_c - T) \quad (14)$$

and the temperature dependence of the soft-mode frequency below  $T_c$  has the form

$$\nu_0^2 = (2/M)\beta_1\rho^2 = (2\lambda/M)(\beta_1/\gamma_1)(T_c - T). \quad (15)$$

If, however,  $\gamma_1^2 \ll 4\lambda G(T_c - T)$ , then the phase transition is close to the triple point. In this case the order parameter will have a different temperature dependence:

$$\rho^2 = [\lambda(T_c - T)/G]^{1/2}. \quad (16)$$

The temperature dependence of the soft-mode frequency at temperatures  $T < T_c$  in this case will have the form

$$\begin{aligned} \nu_0^2 &= (4\lambda/M)\{(\beta_1/\lambda^2)(4G/\lambda^3)^{-1/2}(T_c - T)^{1/2} \\ &\quad + (T_c - T)\}. \quad (17) \end{aligned}$$

At temperatures  $T > T_c$  the behavior of the soft-mode frequency in the region of where the Landau theory is applicable does not depend on the character of the phase transition and is determined by the formula

$$\omega_{\text{SM}}^2 = (\lambda/M)(T - T_c). \quad (18)$$

Depending on the type of phase transition, the behavior of  $\nu_{\text{SM}}(T)$  at temperatures  $T < T_c$  is of a qualitatively different character [compare Eqs. (15) and (17)]. For a second-order phase transition the temperature dependence of the soft-mode frequency is described by a power-law function with critical exponent  $\beta = 0.5$ . For a phase transition close to the triple point the temperature dependence  $\nu_0(T)$  is determined simultaneously by two terms, which depend on the temperature as  $(T_c - T)^{1/2}$  and  $(T_c - T)^{1/4}$ .

The experimental temperature dependence of the soft-mode frequency in  $\text{Hg}_2\text{Cl}_2$  and  $\text{Hg}_2\text{Br}_2$  at temperatures  $T < T_c$  is described well by a function of the form (9), which fits within the Landau phenomenological theory of phase transitions near the triple point [see Eq. (17)]. This result also agrees with the experimental data<sup>8,9</sup> on the heat capacity  $C_p(T)$  and spontaneous deformation  $\varepsilon(T)$ , for which the following values were obtained for the critical indices:  $\alpha \approx 0.5$  ( $C_p$ ) and  $2\beta \approx 0.5$  ( $\varepsilon$ ).

We now compare the experimental temperature dependence of the soft-mode frequency  $\nu_{\text{SM}}(T)$  (9) in  $\text{Hg}_2\text{Cl}_2$  and  $\text{Hg}_2\text{Br}_2$  crystals with the theoretical curve  $\nu_0(T)$  (17). Note that in Eq. (9)  $b_0 \neq 0$ . This is related, in all probability, with dynamical phenomena (for example, interaction with a relaxation mode). In this case the experimentally observed renormalized soft-mode frequency  $\nu_{\text{SM}}$  is related to the unrenormalized soft-mode frequency  $\nu_{\text{SM}}^0$  by the relation<sup>12</sup>

$$(\nu_{\text{SM}}^0)^2 = \nu_{\text{SM}}^2 - \delta^2, \quad (19)$$

where  $\delta^2$  is the parameter characterizing the interaction of the soft mode with the relaxational mode.

Figure 9 displays the temperature dependence obtained using Eq. (9) of the soft-mode frequency  $\nu_{\text{SM}}^0$  of  $\text{Hg}_2\text{Cl}_2$  (a) and  $\text{Hg}_2\text{Br}_2$  (b) crystals. We assumed  $\delta^2 = b_0$ . The solid line represents the temperature dependence  $\nu_0(T)$ , obtained using the formula (17), where the parameters of the thermodynamic potential were determined by an independent method from the temperature dependence of the heat capacity and spontaneous deformation:<sup>10</sup>  $\beta_1/\lambda^2 = 20 \cdot 10^{18} \text{ K}^2/\text{ergs}$  ( $\text{Hg}_2\text{Cl}_2$ ) and  $19 \cdot 10^{18} \text{ K}^2/\text{erg}$  ( $\text{Hg}_2\text{Br}_2$ );  $G/\lambda^3 = 1.1 \cdot 10^{36} \text{ K}^4/\text{ergs}^2$  ( $\text{Hg}_2\text{Cl}_2$ ) and  $1.7 \cdot 10^{36} \text{ K}^4/\text{ergs}^2$  ( $\text{Hg}_2\text{Br}_2$ ). The quantity  $(\lambda/M) = g^2/T_c$  was determined from the temperature dependence of the soft-mode frequency at the  $X$  point of the Brillouin zone of the paraphase (8). Good agreement is observed between

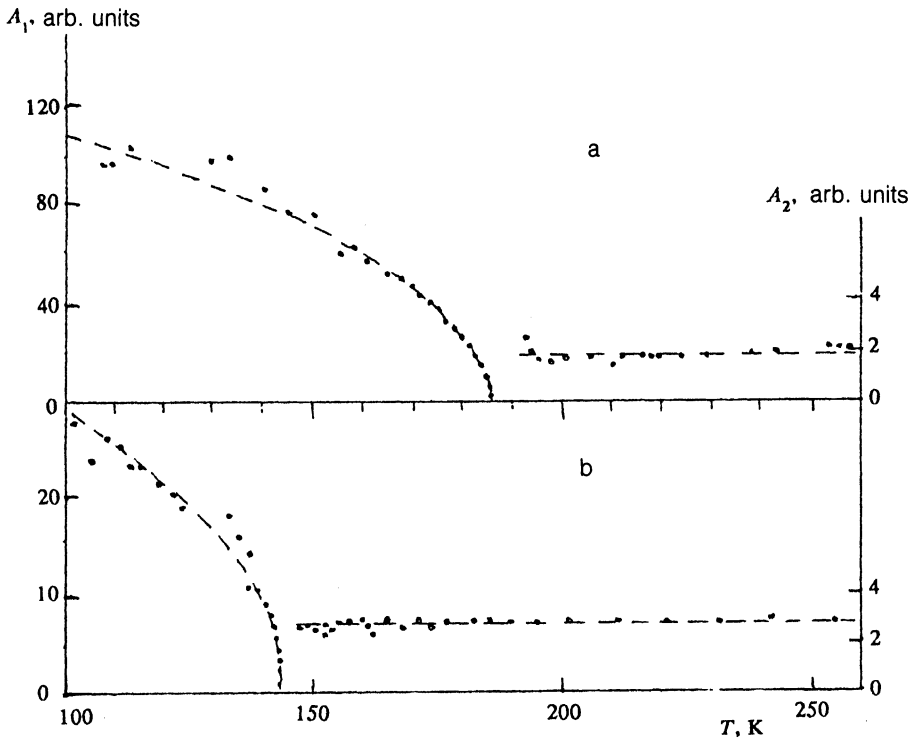


FIG. 10. Temperature dependence of the squared photon-phonon interaction parameter  $A_1$  ( $T < T_c$ ) and the parameter  $A_2$  ( $T > T_c$ ) of  $\text{Hg}_2\text{Cl}_2$  (a) and  $\text{Hg}_2\text{Br}_2$  (b) crystals. The points are the experimental data and the dashed line was computed theoretically.

the temperature dependence  $\nu_{\text{SM}}^0(T)$  and the theoretical curve; this indicates that the phase transition in  $\text{Hg}_2\text{X}_2$  occurs near the triple point.

In order to compare the experimental results for the soft-mode intensity above  $T_c$  with the results of the Landau phenomenological theory, the temperature dependence  $A_2 \sim (I_x^{\text{int}} \omega_x) / T^2$  [see Eq. (7)] is displayed in Fig. 10. This quantity remains constant, as predicted by the theory, over a wide temperature interval.

The character of the temperature dependence of the squared order parameter can be determined by analyzing the soft-mode intensity below  $T_c$ . Since first-order Raman scattering by the soft mode in the paraphase of calomel is forbidden by the selection rules, the relation between the dielectric permittivity  $\epsilon$  of the crystal and the order parameter  $\rho$  is determined by a quadratic law  $\Delta\epsilon \sim \rho^2$ . Taking this fact into account and representing  $\rho$  as a sum of the static order parameter  $\rho_0$  and the dynamic component  $\rho_d$ , we can easily show that  $A_1 \sim \rho_0^2$ . Figure 10 displays the temperature dependence  $A_1 \sim (I_{\text{SM}}^{\text{int}} \nu_{\text{SM}}^2) / T$ . The figure also displays (dashed line) the temperature dependence  $\rho_0^2 \sim (T_c - T)^{1/2}$  "normalized" appropriately. It is observed that the experimental values agree qualitatively with the theoretical temperature dependence; this confirms the conclusion that the phase transition in  $\text{Hg}_2\text{Cl}_2$  and  $\text{Hg}_2\text{Br}_2$  occurs close to the triple point.

The ratio of the intensities of the first and second order soft-mode RSS also makes it possible to estimate the range of applicability of the Landau theory. According to Ref. 12, in the critical region these intensities must be of the same order of magnitude. According to our estimates, this region is of the order of 0.1–1 K, which agrees with the

estimate obtained in Ref. 10 from the Levanyuk–Ginzburg criterion.

As has already been mentioned above, as  $T \rightarrow T_c^-$  the experimentally observed frequency  $\nu_{\text{SM}}$  in  $\text{Hg}_2\text{X}_2$  does not approach zero (Figs. 3A, B (a), and 5), as the Landau phenomenological theory requires [see Eq. (17)], but rather reaches some finite value  $\nu_{\text{min}}$ —it "saturates" ( $\nu_{\text{min}} \sim 3.5 \text{ cm}^{-1}$  for  $\text{Hg}_2\text{Cl}_2$  and  $\nu_{\text{min}} \sim 2.5 \text{ cm}^{-1}$  for  $\text{Hg}_2\text{Br}_2$ ).<sup>2)</sup> The "saturation" of the soft-mode frequency as  $T \rightarrow T_c^-$  is due, in all probability, to the interaction of the order parameter of  $\text{Hg}_2\text{X}_2$  with a relaxational mode. Experiments on neutron scattering in  $\text{Hg}_2\text{Cl}_2$  have shown<sup>7</sup> that as  $T \rightarrow T_c^+$  a central peak is observed together with the soft mode from the  $X$  point of the Brillouin zone of the paraphase. This is one manifestation of the interaction with the relaxation mode whose interaction parameter is  $\delta^2$  at the phase transition point  $\delta^2 = \omega_{\text{min}}^2 \sim 0.035 \text{ (meV)}^2$ . In all probability this can explain the deviation of the experimental values of the frequency  $\omega_X$  near the phase-transition point ( $T > T_c$ ) (see Fig. 4) from the theoretical relation (18), which neglects the interaction with the relaxational mode.

The anomalous behavior of the intensity near the phase-transition point can also be explained, in all probability, by the interaction of the soft mode with a relaxation mode, since as the phase-transition point is approached  $\rho^2 \rightarrow 0$  and  $\nu_{\text{SM}}^2 \rightarrow \nu_{\text{min}}^2 \neq 0$ .

In conclusion, we note that according to Refs. 2 and 3  $\nu_{\text{SM}} \sim (T_c - T)^\beta$ , where  $\beta \approx 1/3$ . This value of the critical exponent  $\beta$  arises because the experimental temperature dependence  $\nu_{\text{SM}}(T)$  (9), which is determined simultaneously by two terms depending on the temperature as



$(T_c - T)^{1/2}$  and  $(T_c - T)^{1/4}$ , can easily be approximated by a power-law function with a value of  $\beta$  close to 1/3. Another possible explanation of this behavior of the soft-mode frequency is the effect of critical fluctuations. It should be noted, however, that in this case the fluctuations should result in the same change in the temperature dependence of the soft-mode frequency both above and below the phase-transition point. The experimentally observed functions  $\nu_{SM}(T)$  and  $\omega_X(T)$  have completely different power-law dependences (8,9). In addition, if the temperature dependence  $\nu_{SM}(T)$  below  $T_c$  is due to critical fluctuations in the entire measured temperature range, then this would necessarily result in strong damping of the soft mode in this temperature interval. However, anomalous behavior of the soft-mode damping constant  $\Gamma_{SM}(T)$  is observed only close to the phase-transition point (Fig. 5). If fluctuations are critical, then the temperature dependence  $\nu_{SM} = (T - T_c)^\beta$  for  $T < T_c$  should follow a power law with exponent  $\beta > 0.5$  (Ref. 12), which is not observed experimentally. In addition, in the critical region the intensities of the first- and second-order soft-mode RSS should be comparable in magnitude. The experimentally observed ratio of the soft-mode intensities in  $Hg_2X_2$  below and above  $T_c$  indicates that the critical region in monovalent mercury halides is quite narrow.

Thus, the obtained experimental data can be described successfully within a phenomenological theory, assuming that the phase transition in monovalent mercury halides occurs near the triple point. The model proposed for the phase transition explains the temperature dependences of the soft-mode frequency and the temperature dependences of the RSS intensity above and below the phase-transition temperature. The shape of the second-order RSS line is described successfully on the basis of a quadratic phonon

dispersion law near the  $X$  point of the Brillouin zone.

We thank A. A. Kaplyanskii, A. P. Levanyuk, V. S. Vikhnin, and A. K. Tagantsev for fruitful discussions and for their interest in this work.

<sup>1)</sup>The soft mode at the center of the Brillouin zone of the ferroelectric phase of  $Hg_2X_2$  is denoted by  $\nu_{SM}$ , in contrast to  $\omega_{SM}$  which denotes the soft mode from the boundary of the Brillouin zone of the paraphase.

<sup>2)</sup>This fact explains the existence of a "gap," observed in Ref. 4, between the combination soft-mode tone  $\omega_{4,5} = \nu_2^\pm \pm \nu_{SM}$  and the fundamental vibration  $\nu_2^\pm$  at  $T = T_c$  in the RSS of  $Hg_2X_2$ .

<sup>1</sup>A. A. Kaplyanskii, Yu. F. Markov, and Ch. Barta, *Izv. Akad. Nauk SSSR, Ser. Fiz.* **43**, 1641 (1979).

<sup>2</sup>Ch. Barta, A. A. Kaplyanskii, V. V. Kulakov, and Yu. F. Markov, *Pis'ma Zh. Eksp. Teor. Fiz.* **21**, 121 (1975) [*JETP Lett.* **21**, 54 (1975)].

<sup>3</sup>Ch. Barta, A. A. Kaplyanskii, V. V. Kulakov, V. Z. Malkin, and Yu. F. Markov, *Zh. Eksp. Teor. Fiz.* **70**, 1429 (1976) [*Sov. Phys. JETP* **43**, 744 (1976)].

<sup>4</sup>B. S. Zadokhin, A. A. Kaplyanskii, and Yu. F. Markov, *Fiz. Tverd. Tela* **22**, 2659 (1980) [*Sov. Phys. Solid State* **22**, 1552 (1980)].

<sup>5</sup>B. S. Zadokhin, A. A. Kaplyanskii, M. F. Limonov, and Yu. F. Markov, *Fiz. Tverd. Tela* **29**, 187 (1987) [*Sov. Phys. Solid State* **29**, 103 (1987)].

<sup>6</sup>M. E. Boiko and A. A. Vaipolin, *Fiz. Tverd. Tela* **19**, 1903 (1977) [*Sov. Phys. Solid State* **19**, 1117 (1977)].

<sup>7</sup>I. P. Benoit, G. Hauret, and I. Lefebvre, *J. Physique (Paris)* **43**, 641 (1982).

<sup>8</sup>B. S. Zadokhin, A. A. Kaplyanskii, B. Z. Malkin, and Yu. F. Markov, *Fiz. Tverd. Tela* **22**, 1555 (1980) [*Sov. Phys. Solid State* **22**, 910 (1980)].

<sup>9</sup>Ch. Barta, V. P. Zhigalov, B. S. Zadokhin, and Yu. F. Markov, *Fiz. Tverd. Tela* **33**, 2739 (1991) [*Sov. Phys. Solid State* **33**, 1548 (1991)].

<sup>10</sup>M. E. Boiko, Yu. F. Markov, V. S. Vikhnin, A. S. Yurkov, and B. S. Zadokhin, *Ferroelectrics* **130**, 263 (1992).

<sup>11</sup>A. A. Kaplyanskii, Yu. F. Markov, and V. Yu. Mirovitskii, *Fiz. Tverd. Tela* **29**, 3625 (1987) [*Sov. Phys. Solid State* **29**, 2076 (1987)].

<sup>12</sup>H. Z. Cummins and A. P. Levanyuk [Eds.], *Light Scattering Near Phase Transitions*, North-Holland Publishing Co., N.Y., 1983.

Translated by M. E. Alferieff